Simvastatin Impairs Hippocampal Synaptic Plasticity and Cognitive Function in Mice

Yujun Guo
University of Science and Technology of China
Guichang Zou
University of Science and Technology of China
Jin Jin
University of Science and Technology of China
Lei Yao
University of Science and Technology of China
Keke Qi
University of Science and Technology of China
Yang Pan
University of Science and Technology of China
Wei Xiong (wxiong@ustc.edu.cn)
Department of Neurosurgery, Institute on Aging and Brain Disorders, The First Affiliated Hospital of USTC, Division of Life Sciences and Medicine, Hefei National Laboratory for Physical Sciences at the Microscale, University of Science and Technology of China, Hefei 230026, China

---

Research

Keywords: Simvastatin, Cholesterol, Hippocampus, Cognition, Mass spectrometry imaging

Posted Date: September 18th, 2020

DOI: https://doi.org/10.21203/rs.3.rs-76680/v1

Version of Record: A version of this preprint was published on February 24th, 2021. See the published version at https://doi.org/10.1186/s13041-021-00758-x.

Abstract

Lipophilic statins which are blood brain barrier (BBB) permeable are speculated to affect the cholesterol synthesis and neural functions in the central nervous system. However, whether these statins can affect cholesterol levels and synaptic plasticity in hippocampus and the *in vivo* consequence remain unclear. Here, we report that long-term subcutaneous treatments of simvastatin significantly impair mouse hippocampal synaptic plasticity, reflected by the attenuated long-term potentiation of field excitatory postsynaptic potentials. The simvastatin administration causes a deficiency in recognition and spatial memory but fails to affect motor ability and anxiety behaviors in the mice. Mass spectrometry imaging indicates a significant decrease in cholesterol intensity in hippocampus of the mice receiving chronic simvastatin treatments. Such effects of simvastatin are transient because drug discontinuation can restore the hippocampal cholesterol level and synaptic plasticity and the memory function. These findings may provide further clues to elucidate the mechanisms of neurological side effects, especially the brain cognitive function impairment, caused by long-term usage of BBB-permeable statins.

Introduction

Statins are the most effective low density lipoprotein-cholesterol lowering medications by targeting 3-Hydroxy-3-methylglutaryl coenzyme A (HMG-CoA) reductase in blood and liver (1, 2). Statins have widely been recognized as the first-line medications for the therapy of strokes and cardiovascular diseases for years (3, 4). Various types of statins including atorvastatin, lovastatin, rosuvastatin and simvastatin have been approved by the U.S. Food and Drug Administration (FDA) (5). According to their capacity to cross the blood-brain barrier (BBB), statins are classified as lipophilic statins including atorvastatin, simvastatin and lovastatin which are BBB-permeable, and hydrophilic statins including rosuvastatin and pravastatin which are BBB-impermeable (6). Indeed, the lipophilic simvastatin has been reported to significantly reduce brain cholesterol level when compared with hydrophilic pravastatin in mice (7). Clinical studies also showed that atorvastatin and simvastatin usage could cause reversible cognitive function impairment (8, 9). However, the underlying mechanisms upon how statins affect brain cognitive function remain unsolved.

Cholesterol is ubiquitous in the central nervous system (CNS). Accurate maintenance of brain cholesterol level is essential for normal brain function including signaling and synaptic plasticity (10, 11). Brain cholesterol metabolic deficiency has been linked to varieties of neurological disorders, such as Alzheimer's disease, Parkinson's disease and Huntington disease (12–14). Human studies have demonstrated that low levels of total cholesterol are associated with poor performance on cognitive function (15). Animal studies have also reported that animals with cholesterol synthesis deficiency suffer severe declines in learning and memory abilities (16, 17). Dietary cholesterol can improve the performance of rodents in Morris Water Maze (MWM) tests. Such improvement is suggested to be associated with the changes in synaptic plasticity of hippocampus (18, 19).

Hippocampal synaptic structure and function are always linked to brain cognition (20, 21). Hippocampal cholesterol loss may impair brain synaptic functions including electrical or chemical signal transmission and therefore lead to the poor cognition (22–25). Although BBB-permeable statins have been suggested to affect brain cognition, it remains unclear whether they affect cholesterol levels in hippocampus and the hippocampal synaptic plasticity. To answer these questions, here we combined our recently developed desorption electrospray ionization mass spectrometry (DESI-MS) imaging technology (26) with field potential recordings and behavioral tests. Chronic simvastatin treatments indeed significantly reduced long-term potentiation (LTP) in hippocampal slices of mice and impaired their recognition memory. The MS imaging revealed a remarkable down-regulation of cholesterol in hippocampus in simvastatin-treated mice. Furthermore, drug withdrawal significantly restored the hippocampal synaptic plasticity and the memory function of mice, with simultaneous recovery of cholesterol level in hippocampus. These findings provide a basis for studying the neurological and cognitive side effects of BBB-permeable lipophilic statins.

Methods

Animals. All procedures were approved by the Institutional Animal Use and Care Committee of School of Life Sciences, University of Science & Technology of China. Adults C57BL/6 male mice aged 6 weeks were used for all studies. Mice were obtained from Vital River Laboratory Animal Technology Co., Ltd. (Beijing, China). Simvastatin (S.C.) at 30 mg/kg was used. All mice were housed at 18–23℃ with 40–60% humidity under a 12-h dark/light cycle (lights off at 7 p.m) and free access to food and water.

Novel Object Recognition. The open-field apparatus consisted of an acrylic chamber (40 cm × 40 cm × 30 cm). Two different objects were prepared in duplicate: towers of rectangular Lego bricks (built from blue, green and yellow bricks) and circular Lego bricks (built from yellow and red bricks). The objects were placed 10 cm away from the walls and attached to the floor. Mice were tested in the dark (active phase between 7:00 p.m. and 7:00 a.m.). During the familiarization session, mice were allowed to freely explore two identical objects (rectangular Lego) placed into the arena at fixed locations for 3 min. The ANY-maze video-tracking system (Stoelting, Wood Dale, USA), which is based on nose-point detection, was used to record the time spent exploring objects. Active exploration was defined as mice sniffing or touching the object when the gap between the nose and the object was less than 2 cm. Climbing over the object or gnawing the object was not considered as exploratory activity. At the end of the test, each mouse was returned to its home cage, and the chamber and objects were cleaned using 75% ethanol, then air-dried for 3 min. After an intersession interval (ISI) of 24 h, one of the familiar objects was replaced by a novel object (circular Lego). The location of the novel object (left or right) was randomized among the mice and the groups tested. Object preference was calculated by using the following formula: preference % = (time to explore the individual object/total exploration time for both objects) × 100%). Data were excluded if the total of exploration time was less than 10 s.

Morris Water Maze (MWM). The spatial memory ability of mice was measured using MWM test. Mice of each group were trained in a large tank 120 cm in diameter and 40 cm in depth, which was divided into

four quadrants. And a hidden 10-cm-diameter platform, 1 cm below the surface of warm water was placed in the center of one quadrant. The pool was covered with a black curtain with four visual cues on the wall of pool. Water was kept at 20 ° C and opacified with titanium dioxide. The trials were conducted 4 times daily at the same time point for 5 successive days. Mice were placed into four quadrants in order (spaced 20 min apart) to swim freely for a maximum of 60 s. If a mouse did not find the platform within a 60-second period, it was gently guided to the platform and allowed to stay on it for 15 s. The latency to find platform was recorded.

Rotarod Test. The rotarod training system (XR1514, Xinruan, Shanghai, China) was used for Rotarod test. Before the first training sessions, the mice were habituated to stay on a stationary rod for 2 min. A total of six trials for the rotarod test were carried out using an accelerating protocol from 4 to 60 rpm in 300 s with 20-min inter-trial intervals. After falling, the mice were immediately placed back to their home cages and the time to fall was automatically recorded by the rotarod software. Once the trial reached to 300 s, the mice were manually removed from the rod immediately. The apparatus and testing area were cleaned with 75% ethanol (w/v) after each trial.

Open Field Test. Open field test system (XR-XZ301, Xinruan, Shanghai, China) was used. The mice were individually transferred from home cage to the open field room (width, 45 cm; length, 45 cm; height, 45 cm) for locomotion test. The whole experiment lasted for 15 minutes. Locomotor activity was recorded by camera and the distance each mouse travelled was measured by ANY-MAZE software (Global Biotech Inc.).

Elevated Plus Maze. Anxiety and fear were measured using an elevated plus maze apparatus. The apparatus consisted of a cross-shaped maze (with 25 cm × 5 cm arms) elevated by a 60-cm support. Two opposite arms were surrounded by a 20-cm wall, while the other two were open (only with a 1-cm contention step). Mice were individually placed in the central area of the apparatus, facing one of the closed arms, and their mobility within the maze was assessed over 5 min. The exploration profile within the different areas of the maze (open arms, closed arms and center) was analyzed, and anxiety behavior was assessed by examination of the open arm exploration. Animals that fell from the apparatus had to be censored from the analyses. Arm preference was automatically analyzed using the ANYmaze video tracking software.

Hippocampal Slice Preparations and Electrophysiological Recordings. Coronal hippocampal slices (350 μm thick) from adult male mice were prepared with Leica Vibratome in ice-cold cutting solution containing (in mM) 30 NaCl, 26 $NaHCO_3$, 10 Glucose, 194 sucrose, 4.5 KCl, 1.2 NaH_2PO_4, 1 $MgCl_2$ and continuously bubbled with carbogen (95% O_2-5% CO_2). The slices were then recovered at room temperature for 1 hour. Slices were transferred into the recording chamber continuously perfused at 12 ml/min with artificial cerebrospinal fluid (ACSF) at 37 ℃. The constituent of ACSF are the followings: (in mM): 124 NaCl, 4.5 KCl, 1 $MgCl_2$, 2 $CaCl_2$, 1.2 NaH_2PO_4, and 26 $NaHCO_3$, continuously bubbled in carbogen. Long-term potentiation (LTP) was induced by HFS (high frequency stimulation, 100 HZ, 1 s) in the CA3 area. Field excitatory postsynaptic potentials (fEPSPs) were recorded using a glass electrode

(filled with NaCl, 3–6 MΩ) placed into the stratum radiatum of the CA1 area. Signals were amplified (gain 100) and filtered (3 kHz), then digitized (10–100 kHz; National Instruments). After a 20-min baseline period preceded attempted LTP induction, Recordings were continued for at least 50 min following LTP induction. LTP was quantified by comparing the mean fEPSP amplitude over the post period with the mean fEPSP amplitude during the baseline period and calculating the percentage change from baseline. Data were collected and analyzed on or off-line by using pClamp 10.4 software (Molecular Devices, Sunnyvale, CA) software.

paDESI-MSI. The mice were sacrificed after behavioral tests. The brain was immediately removed from the skull and flash frozen in liquid nitrogen for 15 s. the frozen mouse brain was transferred to the cryostat chamber of a Vibratome (VT 1200S, Leica, Germany) at − 20 °C. The brain tissue was cut into 16-μm-thick coronal sections and collected onto clean microscope slides. DESI/PI MSI System consisted of a DESI sprayer, a 2D scanning stage, and a postphotoionization interface. A solvent was infused at a flow rate of 3 μL/min through a DESI sprayer (50 μm i.d. and 150 μm o.d. inner fused silica capillary and a 250 μm i.d. and 350 μm o.d. outer fused silica capillary) and directed onto the surface of a tissue slice with a 53° angle of incidence with the assistance of the nebulizing N2 gas (120 psi). The flow of the solvent was driven by a syringe pump, and the metal needle tip was connected to a high-voltage power supply (3500 V for the positive ion mode and − 4000 V for the negative ion mode). The desorbed compounds were sucked in the heated transfer tube (i.d. 0.5 mm, o.d. 1/16 in.) with a 10° angle of collection, and the un-ionized neutral molecules were ionized in an ionization tube (i.d. 4 mm, o.d. 10 mm) by a coaxially oriented krypton DC discharge vacuum ultraviolet (VUV) lamp, which was positioned to shine toward the exit of the transfer tube. Then the ionized species was transferred into a capillary of mass spectrometer. In order to improve the transfer efficiency, an air-flow assisted transport arrangement was added in this interface, and a pneumatic diaphragm pump (60 L/min, model GM-1.0A, Jinteng Experimental Equipment Co., Ltd., Tianjin, China) was connected to the side port of the ionization tube. In experiments, the transfer tube and ionization tube were kept at 300 °C. Note that the krypton lamp was turned off in the DESI mode and turned on in the DESI/PI mode. All imaging data were collected on an Agilent 6224 Accurate-Mass TOF mass spectrometer (Agilent, USA). The flow rate and temperature of drying gas of the mass spectrometer were set at 5 L/min and 325 °C, respectively. A programmable motorized X-Y scanning stage (GCD- 203050M, Daheng, Beijing, China) was used for tissue imaging, and the scanning process was allowed to be synchronized with the Agilent mass spectrometer data acquisition by the customized stage control software. The sample surface was line scanned in the X direction with a stepper motor at a velocity of 370 μm/s while acquiring mass spectra every 0.5 s. The distance between adjacent scan lines in the Y direction was 200 μm. The acquired multiple scan lines were combined in one data file for ion distribution images by using the freely available standalone version of the MSiReader software. Two brain slices respectively from vehicle and simvastatin group on a microscope slice were scanned at the same time. The cholesterol intensity in simvastatin group were normalized with the slice from vehicle group which on the same microscope slice. There were 18 slices were calculated from 6 mice in each group. The identifications for most of these peaks were facilitated by accurate m/z values, comparison of isotope distribution patterns, and tandem mass spectrometry.

Statistics. In our study, no statistical methods were used to predetermine sample sizes, all experiments and data analysis were conducted in a blinded way. All statistical analyses for in vitro recording and behavioral experiments were performed using Prism7 software (GraphPad). Data were statistically compared by unpaired t test, as indicated in the specific figure legends. Average values are expressed as the mean ± SEM. $P < 0.05$ was considered significant.

Results

Hippocampal LTP is inhibited in simvastatin-treated mice

First, we examined the LTP, a main form of synaptic plasticity that underlies synaptic information storage within the CNS (27), in the hippocampal slices of mice receiving subcutaneous (S.C.) chronic simvastatin administration (30 mg/kg/day, 21 days). Field excitatory postsynaptic potentials (fEPSPs) were recorded in CA1 area in response to the electrical stimulation of Schaffer commissural pathway **(Fig. 1a)**. After setting of stimulating and recording electrodes into hippocampal CA3 and CA1, an input–output curve was constructed by stimulating at intensities ranging from 0.3 mA-0.9 mA. High frequency stimulation (HFS, 100 Hz, 1 s) was used to achieve LTP, before which a 20-min baseline recording was performed. Simvastatin did not alter the basic fEPSP amplitudes during the 20-min baseline recording prior to HFS **(Fig. 1b)**. However, the HFS-induced potentiation of fEPSP was significantly reduced in the simvastatin-treated mice when compared with the vehicle-treated control mice **(Fig. 1b and c)**. These results indicate that chronic simvastatin usage can impair the hippocampal synaptic plasticity.

Chronic simvastatin treatments impair recognition and spatial memory

We next conducted behavioral tests including novel object recognition (NOR) and Morris water maze (MWM) to examine the effects of simvastatin on the development of recognition and spatial memory, both greatly involving the hippocampal synaptic plasticity **(Fig. 2a)**.

For NOR test, mice were adapted to the training room for 30 min. Then, the mice were allowed to freely explore two identical objects (rectangular Lego) placed into the arena at fixed locations for 3 min. After an intersession interval (ISI) of 24 h, one of the original objects was replaced by a novel object (circular Lego) and the object preference was calculated **(Fig. 2b)**. The mice spent significantly more time exploring the novel object compared with the familiar object in vehicle-treated mice. Such effect was abolished in simvastatin-treated mice, indicating the deficiency in recognition memory **(Fig. 2b)**.

For MWM test, mice were required to find a hidden platform to escape from swimming in a pool of water. The pool contained four quadrants and the mice were placed into four quadrants orderly (20-min interval) to swim freely for a maximum of 60 s. Four consecutive trials were conducted daily at the same time point for five successive days. Simvastatin-treated mice showed an increased latency to find the platform compared with vehicle-treated mice over the five-day training period **(Fig. 2c)**, indicating the deficiency in spatial memory.

We further examined the effects of simvastatin on other neurological behaviors. Simvastatin did not affect locomotor activity and motor coordination of mice, reflected by unchanged travel distance in the open field tests and unaltered time to fall in the rotarod tests **(Fig. 2d and e)**. In the elevated plus maze test, time spent in the open and closed arms was not changed in the simvastatin treated mice compared with the vehicle-treated mice **(Fig. 2f)**.

Chronic simvastatin treatments reduce cholesterol levels in hippocampus

To examine whether long-term usage of the BBB-permeable simvastatin affects the hippocampal cholesterol level, we used our recently developed paDESI-MS imaging technique (26) to quantify the intensity of cholesterol in the hippocampus of mouse brain sections **(Fig. 3a and b).** The paDESI-MS technique combines conventional DESI with a postphotoionization. The advantage of this technology is that it enhances the ionization and imaging of desorbed neutral molecules such as cholesterol in biological tissue sections. Considering that it will take a long time for paDESI-MS to scan a whole brain slice and may cause degradation of metabolites, in this study we only screened and analyzed a small brain area containing the hippocampus **(Fig. 3c)**. Long-term simvastatin administration significantly reduced brain cholesterol concentration in the hippocampus of mice. There was a strong correlation between hippocampal cholesterol intensities with the recognition memory **(Fig. 3d)** and the spatial memory of mice **(Fig. 3e)**. Taken together, these results suggest that the simvastatin-induced synaptic plasticity impairment and cognition deficiency are correlated with the down-regulation of cholesterol level in hippocampus.

Simvastatin discontinuation restores hippocampal cholesterol levels, synaptic plasticity and memory

For investigating whether the neurological side effects of simvastatin are reversible, the medication was then weaned over a 4-week period in the simvastatin-treated mice. After that, the hippocampal cholesterol levels, LTP amplitude and the memory capacity were all re-examined in these mice. The hippocampal cholesterol concentration was restored to normal level testified by paDESI-MS imaging **(Fig. 4a)**. Both the simvastatin-impaired recognition memory and spatial memory were significantly restored after simvastatin discontinuation **(Fig. 4b and c)**. In addition, the LTP of fEPSP amplitudes in hippocampal CA1 slices were also recovered **(Fig. 4d and e)**. These results suggest that the simvastatin-induced impairment of hippocampal cholesterol, synaptic plasticity and memory is transient and reversible.

Discussion

Statins are widely known as a type of medications lowering low-density lipoprotein (LDL) cholesterol which is always referred to as bad cholesterol (28). Emerging evidences suggest that statins may affect brain cognitive function (8,29). However, the underlying mechanism is still poorly understood. The data presented in this study provides several lines of evidence that BBB-permeable simvastatin may impair cognition via reducing hippocampal cholesterol. First, Long-term simvastatin treatment causes a significant reduction in hippocampal LTP, and the inferior performance of MWM and NOR tests. Second, simvastatin indeed reduces hippocampal cholesterol concentration. The hippocampal cholesterol levels are well correlated with the memory functions of mice. Third, cholesterol discontinuation reverses the

negative effects of simvastatin on hippocampal cholesterol level and synaptic plasticity. These results together suggest simvastatin may impair cognitive function by reducing cholesterol concentration in hippocampus. More importantly, the present study may provide some guiding significance for clinical practice. Although the effects of simvastatin are transient, patients requiring long-term usage of statins should select the BBB-impermeable drugs whenever possible, especially for patients with cognitive disorders.

In the present study, the paDESI-MS imaging technique is introduced to directly measure cholesterol concentration in hippocampus (26). Generally, the cholesterol levels in biological tissues are determined usually by indirect measurements, such as classical chemical methods, enzymatic assay and analytical instrumental approaches including gas and liquid chromatography (30). Compared with the conventional approaches, the paDESI-MS imaging exhibits several unique advantages. First, the paDESI-MS enable detecting cholesterol directly rather than indirectly measuring the H_2O_2 yielded from the oxidase-mediated oxidization of cholesterol (31). Second, the MS imaging achieves the *in-situ* detection of cholesterol in specific subregions of the brain, allowing us to specifically measure cholesterol in hippocampus without interference from cholesterol-rich regions close to the hippocampus such as the corpus callosum. Thus, the paDESI-MS imaging is a powerful technique for qualitative and quantitative analysis of brain cholesterol.

Except for hippocampus, other brain regions may also be affected by simvastatin. Although our MS imaging tests only focus on the hippocampal brain area, cholesterol reduction in white matter and a few brain regions adjacent to hippocampus such as corpus callosum is also observed. Considering this, simvastatin may also affect other neurological functions such as motor and emotion. However, our present results indicate that simvastatin has no effects on motor ability and anxiety behaviors of mice. This is consistent with the clinical studies that no side effects on motor function and emotional states have been observed in patients treated with statins (32-37). These negative results can be attributed to several reasons. For example, simvastatin may have a weaker cholesterol lowering effects in the brain regions related to motor function and emotional regulation when compared with the hippocampus. In addition, the compensation pathways for cholesterol synthesis in these brain regions may be activated after simvastatin administration. Thus, future studies should focus on the heterogeneity among different brain regions in cholesterol synthesis and metabolism.

Statins including lipophilic statins and hydrophilic statins have different capacity to cross the BBB (6). Cholesterol in the brain is locally synthesized independent from peripheral circulating cholesterol due to the presence of BBB (11,38,39). Thus, BBB-permeable lipophilic statins may affect brain cholesterol synthesis and corresponding neurological functions. The present study shows that simvastatin reduces hippocampal cholesterol level and impairs hippocampal synaptic plasticity and memory function. Indeed, hippocampal cholesterol has been found to be correlated with learning and memory (19,22,40). Increased cholesterol efflux impairs hippocampal synaptic plasticity and causes neurodegeneration (22). Hippocampal cholesterol reduction impairs brain synaptic plasticity and leads to cognition impairment (23-25). In addition, LTP formation has been evidenced to be mediated by many synaptic membrane

proteins such as voltage-gated K^+ channels, Na^+ channels and Ca^{2+} channels, NMDA receptors and AMPA receptor (40-46). Cholesterol has been widely reported to modulate the function of these ion channels (41,45,46). Thus, simvastatin may affect the synaptic membrane fluidity and the function of ion channels in the synaptic membrane by lowering hippocampal cholesterol synthesis.

Declarations

Acknowledgements

Not applicable

Authors' contributions

W.X. initiated, designed and supervised the project; Y.G, J.J. and L.Y. conducted behavioral tests and electrophysiological recordings; Y.G., K.Q. and Y.P. conducted mass spectrum imaging; G.Z. and W.X. analyzed data; W.X. and G.Z. wrote the manuscript. The authors read and approved the final manuscript.

Funding

This work was supported by funding from National Natural Science Foundation of China (Grants 91849206, 91649121, 81901157, 91942315), the Strategic Priority Research Program of the Chinese Academy of Sciences (Grant XDB39050000), Key Research Program of Frontier Science (CAS, Grant No. ZDBS-LY-SM002), CAS Interdisciplinary Innovation Team (JCTD-2018-20), National Key R&D Program of China (2016YFC1300500-2), China Postdoctoral Science Foundation (2020TQ0314), the Fundamental Research Funds for the Central Universities, the Major Program of Development Foundation of Hefei Center for Physical Science and Technology (2017FXZY006) and Users with Excellence Program/Project of Hefei Science Center CAS (2019HSC-UE006).

Availability of data and materials

All data in the current study are available from the corresponding author on reasonable request.

Ethics approval and consent to participate

All procedures were conducted in accordance with the animal care standard of the Institutional Animal Use and Care Committee of School of Life Sciences, University of Science & Technology of China.

Consent for publication

Not applicable.

Competing interests

The authors declare no competing interests.

Author details

[1] Department of Neurosurgery, Institute on Aging and Brain Disorders, The First Affiliated Hospital of USTC, Division of Life Sciences and Medicine, Hefei National Laboratory for Physical Sciences at the Microscale, University of Science and Technology of China, Hefei 230026, China. [2] National Synchrotron Radiation Laboratory, University of Science and Technology of China, Hefei 230029, China. [3] Advanced Innovation Center for Human Brain Protection, Capital Medical University, Beijing 100070, China. [4] Center for Excellence in Brain Science and Intelligence Technology, Chinese Academy of Sciences, Shanghai 200031, China

References

1. Tobert JA. Lovastatin and beyond: The history of the HMG-CoA reductase inhibitors. Nat Rev Drug Discov. 2003;2:517–26.
2. Istvan ES, Deisenhofer J. Structural mechanism for statin inhibition of HMG-CoA reductase. Science. 2001;292:1160–4.
3. Lippi G, Plebani M. Statins for Primary Prevention of Cardiovascular Disease. Trends Pharmacol Sci. 2017;38:111–2.
4. Amarenco P, Tonkin AM. Statins for stroke prevention - Disappointment and hope. Circulation. 2004;109:44–9.
5. Endo A. A historical perspective on the discovery of statins. Proc Jpn Acad Ser B Phys Biol Sci. 2010;86:484–93.
6. Ward NC, Watts GF, Eckel RH. Statin Toxicity Mechanistic Insights and Clinical Implications. Circ Res. 2019;124:328–50.
7. Thelen KM, Rentsch KM, Gutteck U, Heverin M, Olin M, Andersson U, von Eckardstein A, Bjorkhem I, Lutjohann D. Brain cholesterol synthesis in mice is affected by high dose of simvastatin but not of pravastatin. J Pharmacol Exp Ther. 2006;316:1146–52.
8. McDonagh J. Statin-related cognitive impairment in the real world: you'll live longer, but you might not like it. JAMA Intern Med. 2014;174:1889.
9. King DS, Wilburn AJ, Wofford MR, Harrell TK, Lindley BJ, Jones DW. Cognitive impairment associated with atorvastatin and simvastatin. Pharmacotherapy. 2003;23:1663–7.
10. Vance JE. Dysregulation of cholesterol balance in the brain: contribution to neurodegenerative diseases. Dis Model Mech. 2012;5:746–55.
11. Zhang J, Liu Q. Cholesterol metabolism and homeostasis in the brain. Protein Cell. 2015;6:254–64.
12. Karasinska JM, Hayden MR. Cholesterol metabolism in Huntington disease. Nat Rev Neurol. 2011;7:561–72.

13. Sun JH, Yu JT, Tan L. The role of cholesterol metabolism in Alzheimer's disease. Mol Neurobiol. 2015;51:947–65.
14. Huang X, Sterling NW, Du G, Sun D, Stetter C, Kong L, Zhu Y, Neighbors J, Lewis MM, Chen H, Hohl RJ, Mailman RB. Brain cholesterol metabolism and Parkinson's disease. Movement disorders: official journal of the Movement Disorder Society. 2019;34:386–95.
15. Elias PK, Elias MF, D'Agostino RB, Sullivan LM, Wolf PA. Serum cholesterol and cognitive performance in the Framingham Heart Study. Psychosom Med. 2005;67:24–30.
16. Schreurs BG. The effects of cholesterol on learning and memory. Neurosci Biobehav Rev. 2010;34:1366–79.
17. Voikar V, Rauvala H, Ikonen E. Cognitive deficit and development of motor impairment in a mouse model of Niemann-Pick type C disease. Behav Brain Res. 2002;132:1–10.
18. Dufour F, Liu QY, Gusev P, Alkon D, Atzori M. Cholesterol-enriched diet affects spatial learning and synaptic function in hippocampal synapses. Brain research. 2006;1103:88–98.
19. Ya BL, Liu WY, Ge F, Zhang YX, Zhu BL, Bai B. Dietary cholesterol alters memory and synaptic structural plasticity in young rat brain. Neurol Sci. 2013;34:1355–65.
20. Reitz C, Brickman AM, Brown TR, Manly J, DeCarli C, Small SA, Mayeux R. Linking Hippocampal Structure and Function to Memory Performance in an Aging Population. Arch Neurol. 2009;66:1385–92.
21. Lisman J, Buzsaki G, Eichenbaum H, Nadel L, Ranganath C, Redish AD. (2018) Viewpoints: how the hippocampus contributes to memory, navigation and cognition (vol 20, pg 1434, 2017). *Nature neuroscience* **21**, 1018–1018.
22. Koudinov AR, Koudinova NV. Essential role for cholesterol in synaptic plasticity and neuronal degeneration. FASEB journal: official publication of the Federation of American Societies for Experimental Biology. 2001;15:1858–60.
23. Martin MG, Pfrieger F, Dotti CG. Cholesterol in brain disease: sometimes determinant and frequently implicated. EMBO Rep. 2014;15:1036–52.
24. Wang D, Zheng W. Dietary cholesterol concentration affects synaptic plasticity and dendrite spine morphology of rabbit hippocampal neurons. Brain research. 2015;1622:350–60.
25. Martin MG, Ahmed T, Korovaichuk A, Venero C, Menchon SA, Salas I, Munck S, Herreras O, Balschun D, Dotti CG. Constitutive hippocampal cholesterol loss underlies poor cognition in old rodents. Embo Mol Med. 2014;6:902–17.
26. Liu CY, Qi KK, Yao L, Xiong Y, Zhang X, Zang JY, Tian CL, Xu MG, Yang JZ, Lin ZK, Lv YM, Xiong W, Pan Y. Imaging of Polar and Nonpolar Species Using Compact Desorption Electrospray Ionization/Postphotoionization Mass Spectrometry. Anal Chem. 2019;91:6616–23.
27. Nabavi S, Fox R, Proulx CD, Lin JY, Tsien RY, Malinow R. Engineering a memory with LTD and LTP. Nature. 2014;511:348-+.

28. Nicholls SJ, Ballantyne CM, Barter PJ, Chapman MJ, Erbel RM, Libby P, Raichlen JS, Uno K, Borgman M, Wolski K, Nissen SE. Effect of two intensive statin regimens on progression of coronary disease. N Engl J Med. 2011;365:2078–87.
29. Chatterjee S, Krishnamoorthy P, Ranjan P, Roy A, Chakraborty A, Sabharwal MS, Ro R, Agarwal V, Sardar P, Danik J, Giri JS, DeGoma EM, Kumbhani DJ. (2015) Statins and Cognitive Function: an Updated Review. *Curr Cardiol Rep* 17.
30. Li LH, Dutkiewicz EP, Huang YC, Zhou HB, Hsu CC. Analytical methods for cholesterol quantification. J Food Drug Anal. 2019;27:375–86.
31. Amundson DM, Zhou M. Fluorometric method for the enzymatic determination of cholesterol. J Biochem Biophys Methods. 1999;38:43–52.
32. Richardson K, Schoen M, French B, Umscheid CA, Mitchell MD, Arnold SE, Heidenreich PA, Rader DJ, deGoma EM. Statins and Cognitive Function. Ann Intern Med. 2013;159:688-+.
33. Mach F, Ray KK, Wiklund O, Corsini A, Catapano AL, Bruckert E, De Backer G, Hegele RA, Hovingh GK, Jacobson TA, Krauss RM, Laufs U, Leiter LA, Marz W, Nordestgaard BG, Raal FJ, Roden M, Santos RD, Stein EA, Stroes ES, Thompson PD, Tokgozoglu L, Vladutiu GD, Gencer B, Stock JK, Ginsberg HN, Chapman MJ, So EA. Adverse effects of statin therapy: perception vs. the evidence - focus on glucose homeostasis, cognitive, renal and hepatic function, haemorrhagic stroke and cataract. Eur Heart J. 2018;39:2526-+.
34. Spindler SR, Li R, Dhahbi JM, Yamakawa A, Mote P, Bodmer R, Ocorr K, Williams RT, Wang YS, Ablao KP. (2012) Statin Treatment Increases Lifespan and Improves Cardiac Health in Drosophila by Decreasing Specific Protein Prenylation. *PloS one* **7**.
35. Hyyppa MT, Kronholm E, Virtanen A, Leino A, Jula A. Does simvastatin affect mood and steroid hormone levels in hypercholesterolemic men? A randomized double-blind trial. Psychoneuroendocrinology. 2003;28:181–94.
36. Morales K, Wittink M, Datto C, DiFilippo S, Cary M, TenHave T, Katz IR. Simvastatin causes changes in affective processes in elderly volunteers. J Am Geriatr Soc. 2006;54:70–6.
37. Stewart RA, Sharples KJ, North FM, Menkes DB, Baker J, Simes J. Long-term assessment of psychological well-being in a randomized placebo-controlled trial of cholesterol reduction with pravastatin. The LIPID Study Investigators. Arch Intern Med. 2000;160:3144–52.
38. Orth M, Bellosta S. (2012) Cholesterol: its regulation and role in central nervous system disorders. *Cholesterol* **2012**, 292598.
39. Pitas RE, Boyles JK, Lee SH, Hui D, Weisgraber KH. Lipoproteins and Their Receptors in the Central-Nervous-System - Characterization of the Lipoproteins in Cerebrospinal-Fluid and Identification of Apolipoprotein-B,E(Ldl) Receptors in the Brain. J Biol Chem. 1987;262:14352–60.
40. Frank C, Rufini S, Tancredi V, Forcina R, Grossi D, D'Arcangelo G. Cholesterol depletion inhibits synaptic transmission and synaptic plasticity in rat hippocampus. Exp Neurol. 2008;212:407–14.
41. Korinek M, Vyklicky V, Borovska J, Lichnerova K, Kaniakova M, Krausova B, Krusek J, Balik A, Smejkalova T, Horak M, Vyklicky L. Cholesterol modulates open probability and desensitization of

NMDA receptors. J Physiol-London. 2015;593:2279–93.
42. Voglis G, Tavernarakis N. The role of synaptic ion channels in synaptic plasticity. Embo Reports. 2006;7:1104–10.
43. Plant K, Pelkey KA, Bortolotto ZA, Morita D, Terashima A, McBain CJ, Collingridge GL, Isaac JTR. Transient incorporation of native GluR2-lacking AMPA receptors during hippocampal long-term potentiation. Nature neuroscience. 2006;9:602–4.
44. Koudinov AR, Koudinova NV. Cholesterol homeostasis failure as a unifying cause of synaptic degeneration. Journal of the neurological sciences. 2005;229:346–7.
45. Levitan I, Singh DK, Rosenhouse-Dantsker A. (2014) Cholesterol binding to ion channels. *Front Physiol* 5.
46. Levitan I, Fang Y, Rosenhouse-Dantsker A, Romanenko V. Cholesterol and ion channels. Subcell Biochem. 2010;51:509–49.

Figures

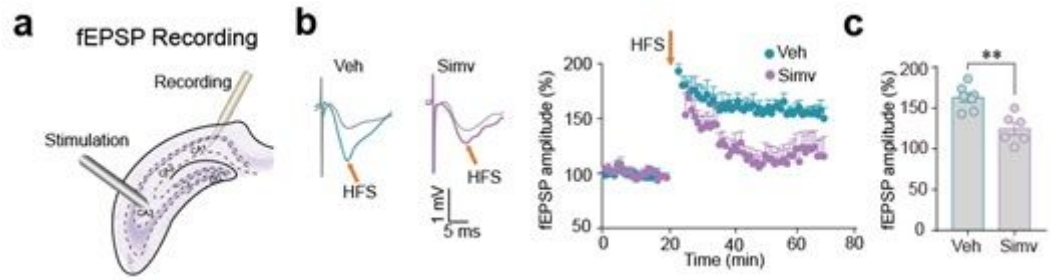

Figure 1

Effects of simvastatin on hippocampal LTP. a Schematic of hippocampal fEPSP recording. b left: representative traces of fEPSPs evoked by electrical stimulation of the Schaffer-commissural projection before and after HFS stimulation in mice treated with chronic vehicle or simvastatin (S.C., 30 mg/kg/day, 21 days). Right: time course of fEPSP amplitudes normalized to baseline. The fEPSP amplitude is plotted as a percentage change against the baseline (20 min) before HFS. HFS: high frequency stimulation. HFS is indicated by arrows. c Normalized fEPSP values (as a percentage of the baseline) in mice treated with chronic vehicle or simvastatin. n=6-7 slices from 3 mice per group. Data are represented as mean ± SEM. **P < 0.01 based on an unpaired t test.

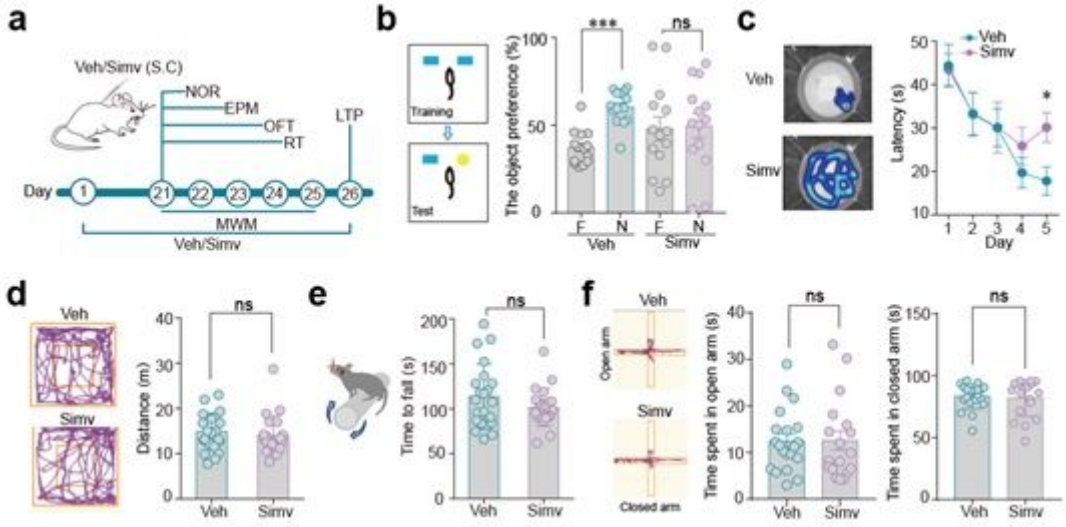

Figure 2

Effect of simvastatin on neurological behavioral performance. a Schematic diagram of simvastatin administration and behavioral tests. MWM: Morris water maze; NOR: Novel object recognition; EPM: Elevated plus maze; OFT: Open field test; RT: Rotarod test. Veh/Simv: Vehicle/Simvastatin. S.C: Subcutaneous. b Left: schematic diagram of Novel object recognition test. Right: average values of time spent in exploring the familiar (F) and the novel objects (N) of mice administrated with vehicle or simvastatin (S.C., 30 mg/kg). c Left: representative heat map traces of mice in the Morris water maze test. Right: time spent in finding the platform of mice administrated with vehicle or simvastatin (S.C., 30 mg/kg). d Left: representative traces of mice in the open field test. Right: average values of the travelling distance of mice in the open field administrated with vehicle or simvastatin (S.C., 30 mg/kg). e Left: schematic diagram of rotarod test. Right: average values of the latency to fall on the rotarod of mice administrated with vehicle or simvastatin (S.C., 30 mg/kg). f Left: representative traces of mice in the elevated plus maze test. Right: average values of the time that mice spent in the open arms and closed arms of the elevated plus maze in mice administrated with vehicle or simvastatin. Data are represented as mean ± SEM. *P < 0.05, ***P < 0.001 based on unpaired t test; ns, not significant (P > 0.05).

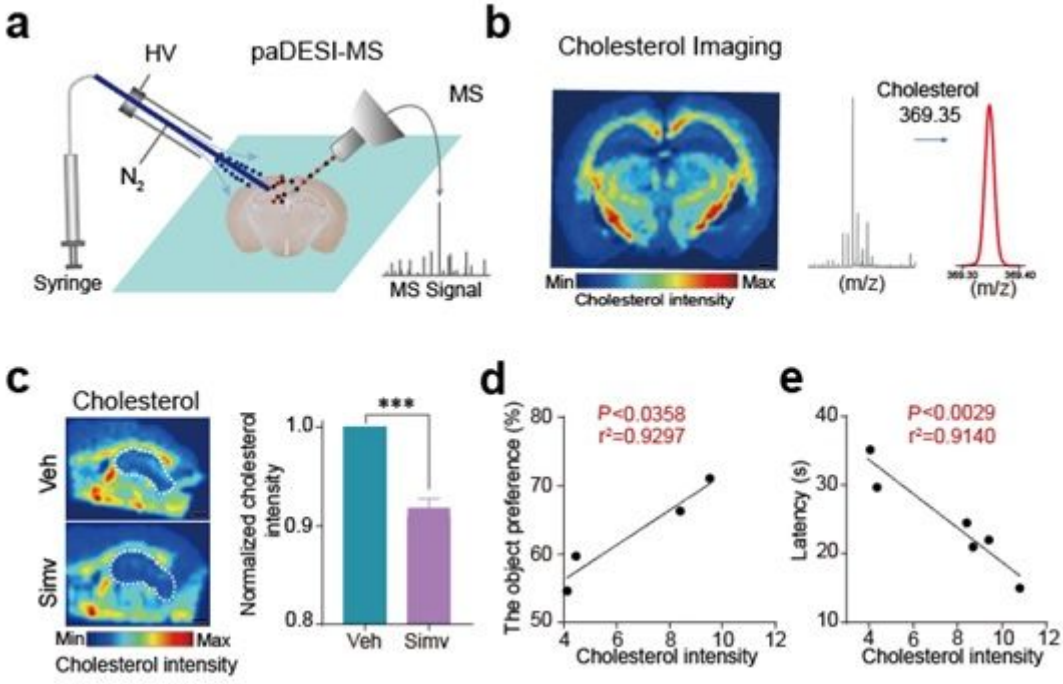

Figure 3

Effect of chronic simvastatin treatments on hippocampal cholesterol level. a Schematic diagram of paDESI-MS imaging setup. b Representative brain cholesterol image and MS spectra of cholesterol obtained from the brain slice. HV, high voltage; N2, nitrogen; MS: mass spectrometry. c Representative brain cholesterol images in mice administrated with vehicle or simvastatin. Normalized brain cholesterol intensity in mice administrated with vehicle or simvastatin. Scale bar: 1 mm. n=6. Simv: simvastatin, Veh: vehicle. d Correlation analysis of hippocampal cholesterol intensity and the novel object preference (%) of mice administrated with vehicle or simvastatin (S.C., 30 mg/kg). e Correlation analysis of hippocampal cholesterol intensity and the latency in finding the platform in mice administrated with vehicle or simvastatin (S.C., 30 mg/kg). n=3-6 mice. Data are represented as mean ± SEM. ***P < 0.001 based on an unpaired t test.

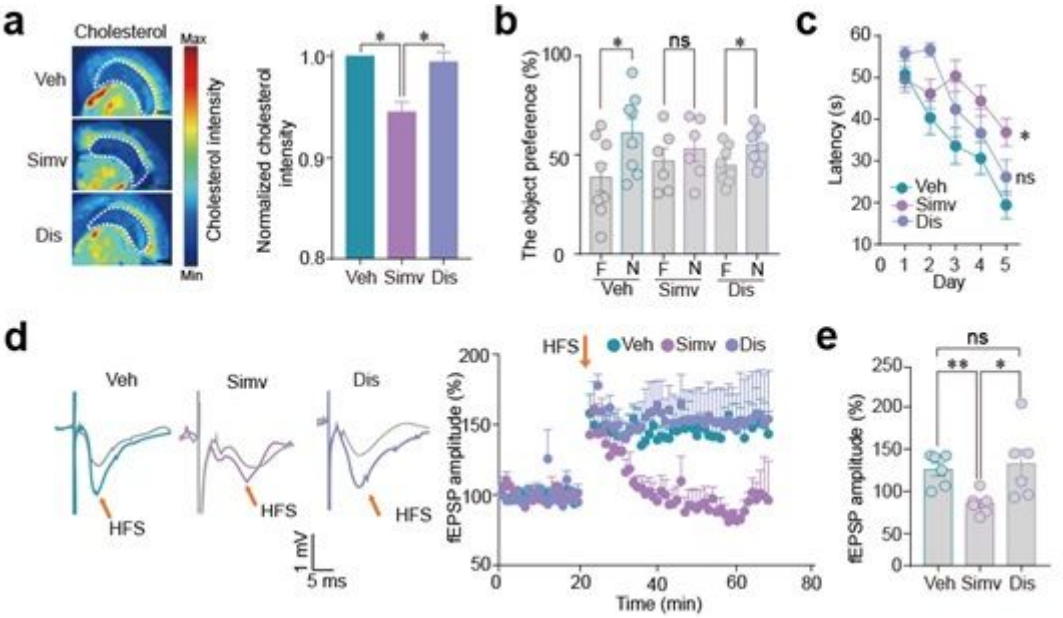

Figure 4

Effects of simvastatin withdrawal on hippocampal cholesterol levels, memory behaviors and hippocampal LTP. a Representative images and normalized intensity of hippocampal cholesterol in mice administrated with vehicle (Veh), simvastatin (Simv) treatments or simvastatin discontinuation (Dis). n=6. Scale bar: 1 mm. b Average values of time spent in exploring the familiar (F) and the novel objects (N) of mice administrated with vehicle, simvastatin or simvastatin-discontinuation. c Latency in finding the platform of mice administrated with vehicle or simvastatin or simvastatin-discontinuation. d left: representative traces of fEPSPs evoked in the CA1 by electrical stimulation of the Schaffer-commissural projection before and after HFS stimulation in mice treated with chronic vehicle or simvastatin or simvastatin-discontinuation. Right: time course of fEPSP amplitudes normalized to baseline. The fEPSP amplitude is plotted as a percentage change against the baseline (20 min) before high-frequency stimulation. HFS is indicated by arrows. e Normalized fEPSP values (as a percentage of the baseline) in mice treated with chronic vehicle or simvastatin or simvastatin-discontinuation. Data are represented as mean ± SEM. *P < 0.05, **P < 0.01 based on unpaired t tests; ns, not significant (P > 0.05).